

# Application of Topology Optimization technique to size the NGCTR-TD engine mount at high temperature using unconventional materials.

Matteo Nigrelli <sup>1</sup>, Giuseppe Sala <sup>2</sup>, Luca Patricelli <sup>1</sup>

<sup>1</sup> Leonardo S.p.A. Helicopters Division

<sup>2</sup> Politecnico di Milano

## Abstract

Within the CS2 FRC framework *Leonardo Helicopters* is leading the team who is going to develop new technologies and solutions for future tiltrotors. The engine mounts turned out to be a design challenge since they have a great impact on the overall weight of the Technological Demonstrator under development and they need to be compliant with very stringent mechanical requirements in a very bad thermal environment (temperatures up to 1100 °C as per certification requirements).

The Topology Optimization technique, using *Optistruct*, was used to investigate a new design of the engine mount of the NGCTR-TD at high temperature. The design guessed was optimized at three different temperatures in the range RT-1000 °C, comparing the use of Stainless steel and Titanium alloy, with the same problem set up to compare the benefits, in terms of mass reduction, of each material.

The results demonstrated that, at temperatures under 538 °C, the introduction of the Titanium alloy guarantees a remarkable mass saving for the current design, but at temperatures above 1000 °C, the benefits obtainable were nullified by the overcoming of the stress constraints, also in areas not subjected to Topology Optimization.

In parallel to this work, the possible benefits of introducing a fire tested thermal coating in the design were investigated through thermal analysis with *Acusolve*, in order to find the most suitable arrangement of layers to protect the structure.

The proposed solution proved to protect the engine mount from high temperatures, reaching on the inside a temperature below 250 °C, thus allowing to investigate the use of Aluminum alloy which is an unconventional choice for this type of application.

After being Topology Optimized and despite of the contribution introduced by the thermal coating, this solution demonstrated to produce the greatest mass saving compared with the other materials, electing the Aluminum alloy to be used for the next stages of the design of the engine mount.

**Keywords:** Topology Optimization, *Optistruct*, Thermal coating.

## 1. Introduction

The aviation industry is a constantly growing sector of excellence in Europe at around 4% per annum[1]. The rapid growth prompts questions of environmental impact and brings new focus on the industry's social obligations. This is where *Clean Sky* comes in.

*Clean Sky* is a European research programme developing innovative, cutting-edge technology aimed at reducing CO<sub>2</sub>, gas emissions and noise levels produced by aircrafts [1].

Funded by the EU's *Horizon 2020* programme, *Clean Sky* contributes to strengthening European aero-industry collaboration, global leadership and competitiveness. The first version of the program was launched in 2008, following increased recognition of the growth of the aviation sector and its implications on the environment.

The 2nd phase of the program was launched in 2014. *Clean Sky 2*, starting from the success of the first one, continues to integrate breakthrough technologies in aircraft and demonstrating innovative configurations of vehicles enabling changes in environmental and economic performance in areas such as Large Passenger Aircraft, Regional Aircraft, Fast Rotorcraft, Airframes, Engines and Systems.

*Leonardo Helicopters* is currently working on the NGCTR-TD project, with the aim of developing an advanced concept for a next generation Tiltrotor. The project goals are the definition of new technologies within an innovative tiltrotor architecture, the main systems and enabling technologies, with the purpose of increasing performance and operational capability with respect to current tiltrotor configurations [2].

The Structural optimization, widely used within *Leonardo Helicopters*, is becoming increasingly important in the functional and technological design of structures. The engineers have to face the difficult task of designing a structure taking into account objectives that are often contradictory, like minimizing the mass, volume, maximize stiffness, minimizing stresses, ensure manufacturability, minimizing costs etc.; the optimization is therefore a multidisciplinary problem. The common design process can be modified including a design optimization, (commonly referred to as Optimization-driven design process) to suggest a design that is much more likely to work; in this way the redesign cycle is all about eliminated [5].

Depending on the type of parameters or design variables chosen, the optimization problem can be classified as Topology, Shaper and Size.

Topology optimization (TO), according to [3], is the most general type of structural optimization; being performed in the initial phases of the design, it has the biggest optimization potential and therefore a major impact on the behaviour of the final structure; offering an initial model that can be fine-tuned afterwards with shape and size optimization methods.

## 2. Requirements and motivation

The Engine mount of the NGCTR-TD, with the task of connecting the engine to the primary structure, in a preliminary stage of the design demonstrated to violate weight requirements with respect to the NTE weight, low accessibility and stress concentrations located at the interfaces with the primary structure. The structure was designed with two pairs or arms, connected laterally to the engine in dedicated points, and joined together before being attached to the primary structure [see *Figure 1*]. Moreover, all the components located in the nacelle, due to the severe temperatures reachable in case of damage, have to withstand with the requirements reported in the ISO 2685[7].

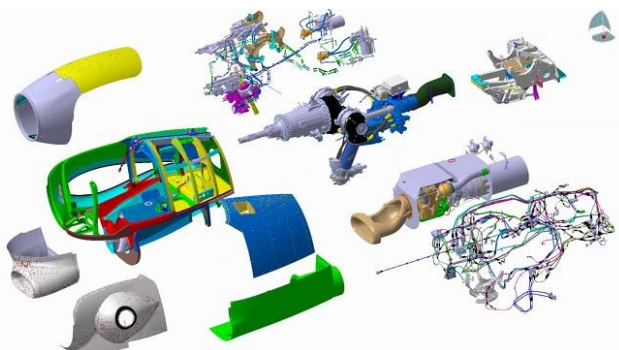


Figure 1 - NGCTR-TD Nacelle Exploded view

77

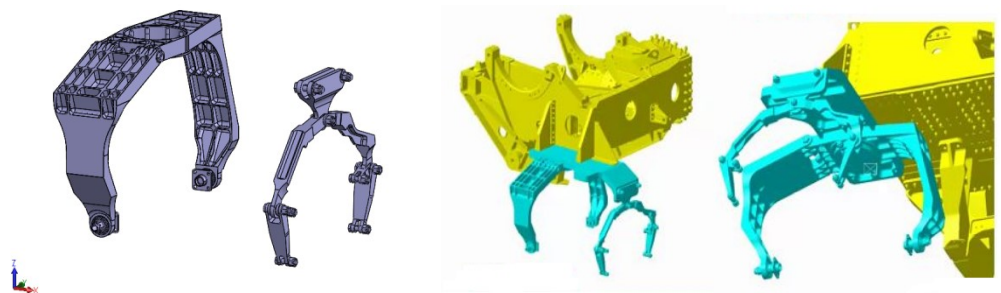


Figure 2 - Preliminary design of the engine mount

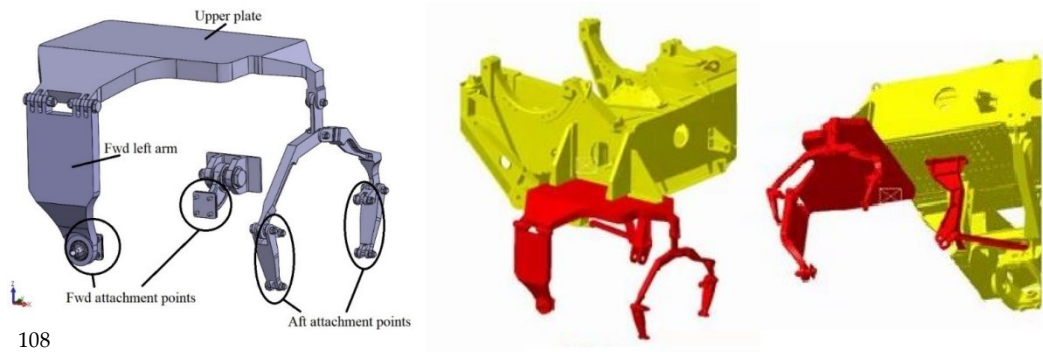
44  
45  
46  
47  
48  
49  
50  
51  
52  
53  
54  
55  
56  
57  
58  
59  
60  
61  
62  
63  
64  
65  
66  
67  
68  
69  
70  
71  
72  
73  
74  
75  
76  
77  
78  
79  
80  
81  
82  
83  
84  
85  
86  
87  
88

The engine mount must prove to be “fireproof” which, according to [7] is the grade of designating components, equipment and structures capable of withstanding the application of heat by a standard flame for 15 min.

The standard flame has the following characteristics:

- Temperature:  $1100\text{ }^{\circ}\text{C} \pm 80\text{ }^{\circ}\text{C}$ .
- Heat flux density received:  $(116 \pm 10)\text{ kW/m}^2$ .

A new design (guess) has been proposed, made of ARMCO® PH 13-8 Mo H1000 stainless steel (called *Baseline* in this work), trying to solve the weak points of the design.



108

109

Figure 3 - New geometry guessed

The new geometry has been achieved starting from the previous model, maintaining unchanged the attachment points and the Aft arms (having demonstrated to be efficient) and splitting the Fwd arms, one directly connected to the engine mount and the other one connected directly to the primary structure with a stand-alone structure, in order to reduce the concentrated stress at the interface with the primary structure and guaranteeing better accessibility to one side of the engine.

The upper plate, initially separated from the rest of the structure, is totally incorporated in the engine mount structure, and in a second time, it will be connected to the primary structure as shown in the following pictures.

The new design is consciously oversized, since the guidelines for the final shape will be provided by the topology optimization.

The isolated Fwd right attachment point is connected to the primary structure (the yellow part in *Figure 3*) by means of metal supports, ensuring rigidity in the three directions, but their design in detail is out of the scope of this work.

The new structure, however, presented a high weight, reaching the 186% of the NTE and here comes the necessity of a structural optimization.

By introducing the Topology optimization in the design loop, unconventional materials and designs have been investigated to find the best solution, in order to reduce the overall weight.

### 3. Methods

The typical approach to plane or volumetric structure topology optimization is the discretization of the problem in finite elements and the assignment of the full material, partial or lack of material to each element, in an iterative scheme converging to the optimal material distribution inside the domain.

The traditional approach to TO with Evolutionary Algorithms (EA), is the discretization of the domain in a grid of FE for the 2D and 3D problems. Each element of the grid has a binary value attached to it (1 for the case when the element is filled with material represented with black square and 0 for the case when the element represents a hole, identified with White Square). A grid of only blacks and whites like the one in the picture is typical only to the so called “hard-kill” methods.

However, other methods employ “soft-kill” techniques, which allow the finite elements to be “gray”, corresponding to “fractional” material; these are usually needed to ensure proper convergence of the algorithm but they are partially eliminated in the final iterations of the procedure, indeed a good check on the result is verifying that not too many fractional density elements are included in the solution.

Since the evolutionary algorithms are population-based and the number of individuals forming the population needs to be of the same magnitude order as the number of optimization parameters (number of grid elements) for the algorithm to converge, applying these methods is extremely expensive from the computational point of view; and in the case of 3D domain the computational costs is even higher. Many solutions to reduce the numbers of fitness evaluations have been proposed such as the generation of the optimal solution over a series of steps as mentioned in [3], each with an increasingly refined grid and with each step starting from the best result of the previous step; however, the TO is a mesh-dependent problem, therefore a more refined mesh will lead to a slightly different design instead of a more refined picture of the previous design [4].

The EA, due to the discrete representation of the domain, leads to connectivity problems; many solutions have been proposed like starting from seed elements (such as the application points of the forces) and considering filled with material only elements connected to these particular points. Another approach recently applied for TO is to use a morphological representation of the geometry, instead the traditional discrete one; the basic primitives used are spline curves or NURBS (Non-uniform rational basis spline) surfaces and some benefits are the optimization carried out directly on the CAD specification tree, where the geometry is represented, and the result itself is a complete final CAD model that doesn't need to be interpreted by the designer as the classic TO outputs.

Nowadays the most studied optimization method, commonly implemented in commercial software, is the SIMP (solid isotropic microstructure with penalization); it is a soft-kill method in which the design volume is divided into a grid on  $N$  elements (isotropic solid microstructures), each element  $e$  having a fractional material density  $\rho_e$  (the design variable). The objective function is the strain energy  $SE$ , under a constraint of target volume  $V^*$ , meaning the technique searches the material density distribution inside the design domain that minimizes strain energy for a preset structure volume.

The densities of the microstructures are gathered in the vector and represent the optimization parameters. Mathematically, the problem can be formulated as:

$$SE(\mathbf{p}) = \sum_{e=1}^N (\rho_e)^p [\mathbf{u}_e]^T [\mathbf{k}_e] [\mathbf{u}_e] \quad 167$$

Subjected to the constraints: 168

$$V^* - \sum_{e=1}^N \rho_e V_e = 0 \quad \mathbf{0} < \rho_{\min} \leq \rho_e \leq 1 \quad 169$$

Where: 170

- $[\mathbf{u}_e]$  represents the nodal displacements vector. 171
- $[\mathbf{k}_e]$  represents the stiffness matrix of element  $e$ . 172
- $\rho_{\min}$  is the minimum allowable density for empty elements, greater than zero to ensure the stability of the finite element analysis. 173

$p$  represents the penalty factor and is the main parameter of the method; its value its needed to diminish the participation of fractional density (grey) elements to the total structural stiffness and to encourage the development of white or black elements; it is normally set equal to 3 and can vary between 2 and 4, otherwise it can be set initially equal to 1 and then increased gradually. 174

The penalization technique used for the density approach is the "power law representation of elasticity properties" which can be expressed for any solid 3-D or 2-D element as follows: 175

$$[\mathbf{k}_e]_p = \rho_e^p [\mathbf{k}_e] \quad 181$$

Where  $[\mathbf{k}_e]_p$  represents the penalized stiffness matrix of the element  $e$ . 182

In order to achieve a stable convergence, design variable changes during each iteration are limited to a narrow range within their bounds, called move limits. Small move limits lead to smoother convergence even if many iterations may be required due to the small design changes at each iteration. Large move limits may lead to oscillations between infeasible designs as critical constraints are calculated inaccurately. 183

The basic SIMP algorithm is reported in *Figure 4*. The starting point is the structure with random density or equal to 1. 184

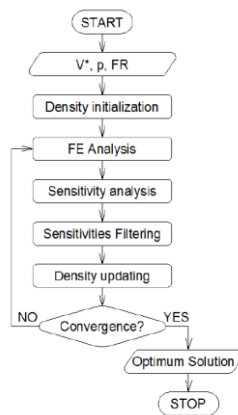


Figure 4 - Flow chart for the SIMP algorithm [3].

The process starts with a FA analysis and the result is used to evaluate the sensitivity of each element (the impact that the variation of the density has on the objective function) in the following form:

$$\frac{\partial SE}{\partial \rho_e} = -p(\rho_e)^{p-1}[\mathbf{u}_e]^T[\mathbf{k}_e][\mathbf{u}_e]$$

At the end, the design update is generated by solving the explicit approximate optimization problem, based on sensitivity information.

It may happen that the calculation of each sensitivity independently, without considering interactions between elements, may lead to discontinuous structures, therefore filtering scheme have been introduced with the aim of averaging the sensitivity of each element considering the weighted influence of all the elements nearby. The sensitiveness is then updated.

A final difficulty to be reported, that may happen, is the non-convexity of the design variable; it is always desirable since a local minimum is, then, also global one. For such problems it is possible that the algorithm terminates to completely different local optima for different starting points. It seems as if engineering intuition must be the guide when a design is accepted. The heuristic methods that may be used include running the problem several times with different starting points or solving several problems where the value of  $q$  is gradually raised from the value 1, which gives a convex problem, to higher values, which give “black and white” designs.

In case technological aspects need to be considered, the algorithm must be modified by imposing supplementary constraints; needless to say, the more technological constraints are considered, the easier it will be to find the final shape, though is not an easy topic since these constraints can’t be accounted by just adopting limits for the design variables.

Within this work, The *HyperWorks suite by Altair* has been used, *OptiStruct* is an industry proven, modern structural analysis solver for linear and nonlinear problems under static and dynamic loadings, used for structural design and optimization. *OptiStruct* generates an optimal design proposal based on a user-defined design space, performance targets, and manufacturing constraints. Topology optimization can be applied to 1-D, 2-D and 3-D design spaces.

*OptiStruct* solves topology optimization problems using the density method, also known as the SIMP method which is a local approximation method to solve the optimization problem.

Since local-based approximation methods (i.e gradient-based optimization methods) are more susceptible of finding a local optimum, while global approximation methods (response surface methods or genetic algorithms) are less susceptible of finding a local optimum, with the release of *OptiStruct* version 11.0, a new global search algorithm called Multiple Starting Points Optimization was made available as an extension to the gradient-based optimization approach. This global search algorithm performs an extensive search of the design space for multiple starting points to improve the chances of finding a more global optimum. In other words, these techniques improve the chances of finding a global optimum. However, no algorithm can guarantee that the optimum found is in fact the global optimum unless the problem is convex.

#### 4. Optimization campaign

A first Optimization campaign, carried on in order to find the guidelines for an optimized shape of the engine mount, has been used to compare the *Baseline* material with a titanium alloy at high temperatures. Within this campaign a reduced set of sizing loads have been use, the only frozen at that stage of the design.

The optimization constraints applied, were referred to the natural frequencies of the structure, to be higher than 10 Hz, in order to avoid resonance problems with the first flapping natural frequency of the wing; to maintain the material within the elastic range and a manufacturing process, in fact ,designs obtained by TO often contain cavities that are not viable for casting therefore *OptiStruct* allows to impose draw direction constraints so that the geometry determined will allow the die to slide in a given direction. These constraints are defined using the DTPL card. In this work the SINGLE draw direction is applied to components A, B, F, G (see *Figure 5*) and the SPLIT option to components C, D, E, H since they present a symmetry in the design.

The choice of the manufacturing process has been done based on the company experience and due to the properties of the materials, indeed, the materials chosen don't present particular problems in machining, except for the required low cutting speed due to the difficulties in removing heat in titanium alloy or to avoid over aging in aluminium alloy.

First the model has been simplified removing internal connections, non-structural chamfer and fittings; then the design volume has been selected, leaving untouched the interface areas; after that the model has been meshed separately with tetrahedral second order elements and the geometrical constraints have been imposed: the internal constraints have been modeled as RBE2, and the external constraints (red areas in *Figure 7* -right) as SPC with 6 d.o.f. blocked.

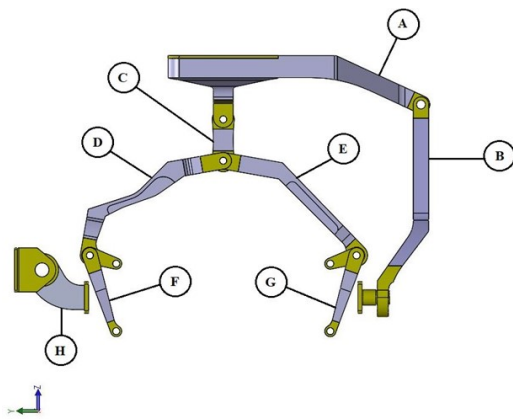


Figure 5 - Untouched parts in the model (green areas)

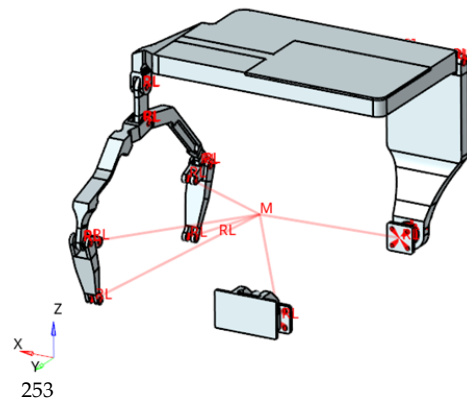


Figure 6 - Engine load connection

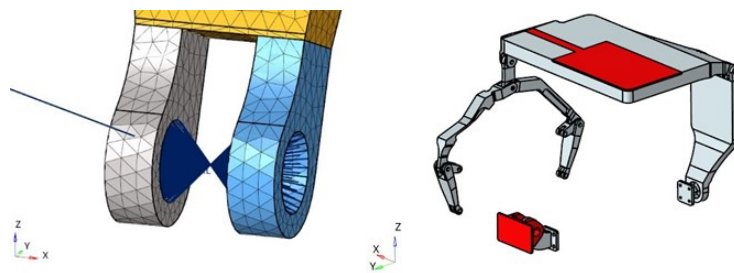


Figure 7 – Internal (left) and external(right) constraints.

The first optimizations are carried out with the same material chosen in the preliminary design phase: ARMCO® PH 13-8 Mo H1000 Stainless Steel, AMS 5864. Other materials normally used by the company in the construction of the airframe are considered, with the aim of reducing the weight of the structure:

- TIMETAL® 6-4, Titanium alloy TI-6Al-4V, AMS 4911( *Sol.2*)
- Aluminum alloy 7050 T7451, AMS 4050 (*Sol.3*)

The optimizations are performed at three different temperatures: at room temperature (24 °C) for which a lot of data is available in the literature, at 538 °C which is the maximum temperature at which the materials have been mechanically tested during tensile tests by the manufacturers and at 1000 °C. The mechanical properties at the highest temperature are measured during compression tests in order to evaluate the manufacturability and they are here used with the hypothesis of isotropic material. However, The Aluminum alloy is not taken into consideration in the first part of the work, because its mechanical properties at high temperature are not comparable with the other materials (*Baseline* and *Sol.2*) and being subjected to sublimation. It will be considered, later on, during the work.

Within this work, the engine mount will be optimized to sustain specific load conditions requested by the company, lower than the maximum sustainable by the engine itself, that are meeting the in-service/landing loads of the NGCTR and certifications requirements.

- Vertical vibrating load: the maximum total vibratory velocity, based on the installation manual of the engine, is modelled with a sinusoidal input along z-axis, applied in the engine's CG, in a range of 60 Hz, with single amplitude peaks equal to 64 mm/sec.
- Torque: the torque transmitted from the engine to the transmission must be balanced by the engine mount. The torque in OEI condition (the most critical) is above 1200 Nm.
- Thrust From exhaust: the residual trust produced by the exhaust gases low compared to the normal thrust produced by the engine, in fact that most of the power is transmitted to the mast.

In addition to the loads reported, coming from the engine, the engine mount has to be sized to sustain the inertia loads produced by the aircraft in flight:

- Vertical discrete load: The mass of the fully built-up engine will be rigidly connected to the engine mounts with the following vertical (top-down) acceleration: 2 g.
- Lateral discrete load: The mass of the fully built-up engine will be rigidly connected to the engine mounts with the following lateral acceleration: 1.33 g.
- Longitudinal discrete load: The mass of the fully built-up engine will be rigidly connected to the engine mounts with the following longitudinal (Backward) acceleration: 1.5 g.

Optimization ID	T [°C]	Material ID	Process Constraint Yes/No
1	24	Baseline	No
2	24	Baseline	Yes
3	24	Sol. 2	Yes
4	538	Baseline	Yes
5	538	Sol. 2	Yes
6	1000	Baseline	Yes
7	1000	Sol. 2	Yes

Table 1 - Summary of optimizations

## 5. Results

In every optimization the most important results are collected; the final geometries, the natural frequencies, the stress and displacement values. By means of the *OSSmooth* function the fractional density elements are converted into full density in order to calculate the mass of the structure, filtering the elements with densities greater than 0.5/0.7/1. Regarding the stresses, safety factors with respect to the yield are computed to verify the structure to be in the elastic field.

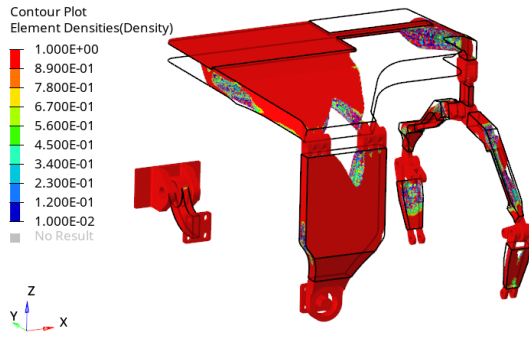


Figure 8 - Optimization 1, global view

Opt. ID	Stress Safety factor	
	Including singularities	Without singularities
1	15.37	16.20
2	14.82	15.30
3	8.76	10.21
4	6.56	7.93
5	4.26	5.38
6	0.88	1.09
7	0.34	0.46

Table 2 - Summary of stress safety factors.

Analysing the data obtained, the main results are reported below:

- The Titanium alloy (*Sol.2*) compared with the *Baseline* at the same temperature, is guaranteeing higher natural frequencies (85% on average) and lower stress safety factors (45% lower on average).
- The first optimization, without manufacturing constraint, is providing higher natural frequencies, with respect the Optimization 2 where the manufacturing constraint is applied, due to the higher stiffness reached by the structure despite of the difficulties in manufacturing.
- Vertical displacements are increasing, comparing optimizations performed with the same material, with the increase in the temperature, due to the considerable reduction in mechanical properties of the material itself.
- Increasing the temperature of the Optimization, with the same material, no significant changes in the final mass are obtained until the constraint on the yield stress is producing effects; this is visible comparing the optimizations performed at 24 °C and at 538 °C where no significant changes are reported, whereas at 1000 °C, the stress constraint is producing a remarkable increase in the final mass.
- The mass saving using *Sol.2* with respect to *Baseline* is steady, increasing temperature, but the structure is not able to support the loads applied within the elastic field; in fact, at 1000 °C the stress safety factor in *Opt. 7*, without considering the values reached on geometrical singularities, is not withstanding the stress constraint on the structure, also in areas not subjected to TO; *Opt.6*, on the other end, shows a thin margin on that constraint.
- The weight of the *Baseline* structure at 1000 °C is equal to 131% of the NTE weight.

## 6. Consideration about the method

A small and not complete set of sizing loads have been used in these optimizations since the goal of this initial campaign was to choose the best material to be used to minimize the mass, at high temperature, of the engine mount, however, the other loads listed previously, will be used later on during this work to guarantee, for example, the ability to counteract lateral, longitudinal and vibrating loads. The design of the engine mount is, indeed, an interdisciplinary subject and needs inputs from different system divisions; furthermore, at the very initial stage of the design, no dynamic loads have been considered because they come from an aircraft level evaluation.

Within these optimizations a small number of elements, with respect to the total number, presented intermediate densities; this aspect can be further mitigated adjusting the discrete parameters (set in the *Opti control panel*) to push elements with intermediate densities toward 1 or 0, and as consequence a more discrete structure is given; an example can be refining the mesh.

Within this campaign has been introduced a minimum volume fraction reachable during the optimization equal to 30%, in fact, without this limit, the solver tended to detach the Aft arms from the rest of the structure.

The highest concentrated stresses after the optimizations are located in the same areas and, as previously mentioned, are overestimating the real stress level due to the presence of elements with intermediate relative densities; further static analysis could be performed after the *OSSmooth* function, but is not useful

since a final design with a CAD is planned to be performed. The same consideration can be done for displacements.

A possible benefit to the design is represented by the movement of the engine mount farther from the fire zone, giving the possibility to change material or, alternatively, by the introduction of a thermal coating able to reduce the temperature perceived by the engine mount.

### 7. Design with thermal coating

The optimizations performed at 538 °C, although useful for understanding the behavior of the material with increasing temperature and the corresponding changes in weight, are not totally accurate and therefore not safe to be considered as final design, since the engine mount must withstand 1100 °C in working conditions; in addition, the optimizations performed at 1000 °C demonstrated the lack in precise data useful for a trustable design.

The idea is to find a thermal coating powerful enough to avoid the engine mount to reach high temperatures and therefore make it possible to use lighter materials, such as the Aluminum alloy (*Sol.3*), unconventional choice for this type of application.

The thermal conductivity and the specific heat of the covering material have been computed according to the ISO 8310 and ISO 11357-4.

The fire test if performed in the laboratory of the company in compliance with the regulation BS ISO 2685, 1998; on a (600\*600\*2) mm sample.

The temperature field measured is reported in the following plot.

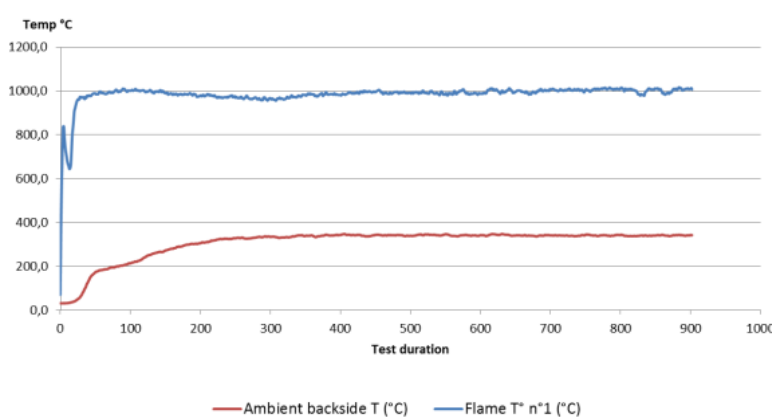


Figure 9 -

Temperature plot during fire test.

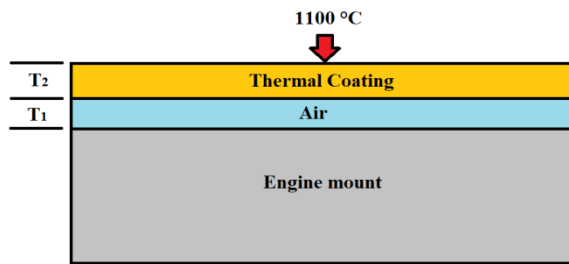
The material has demonstrated to be fireproof, with no significant damages on the flame side. The temperature measured on the hot side is reported in blue, while the temperature on the cold side (in contact with the surface) is reported in red, showing a plateau after 5 minutes around 320 °C.

These results, however, come from a test environment, useful to verify the material behaviour in case of a direct flame, but not fully useful for determining the actual heat transfer in the real system, therefore a numerical analysis of the temperature reached on the components has to be performed.

A numerical simulation of the internal temperature reached in the components covered by the thermal coating, subjected to 1100 °C for 15 minutes, is performed, using *HyperWorksCFD 2020* as preprocessor, *Acosolve* as solver and, in the end, *Hyperview* as postprocessor.

Based on the company experience, the goal of the thermal coating is to reach an internal temperature of the components below 250 °C, to be able to use lighter material with respect to the *Baseline*.

The set-up of the problem is reported by the following scheme: the thermal coating (thickness  $T_2$ ) encloses a layer of air (thickness  $T_1$ ) and the components; the contact condition is imposed between the layers. The outside temperature is imposed to be 1100 °C.



395

Figure 10 - Schematic of the Thermal Analysis. 396

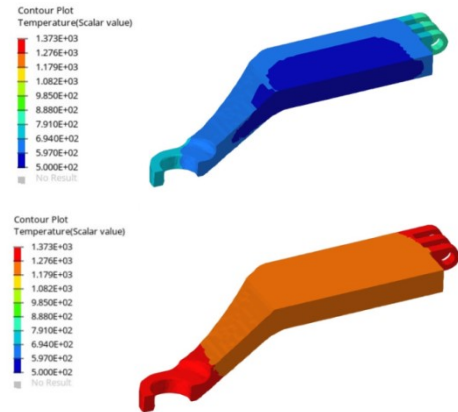


Figure 11 - Temperature [k] after 1 minute during thermal analysis, Baseline material. T1=0, T2 =3 mm (up) and Temperature [k] after 15 minutes during thermal analysis, Baseline material. T1=0, T2 =3 mm (down) 397  
398  
399  
400  
401

The results showed a temperature jump between the inside of the component and the outside temperature; the values have been measured in different points across the component and averaged. 402  
403

A case study with 3 mm thickness of thermal coating shows that the difference in the temperatures reached in the three materials selected( *Baseline*, *Sol. 2*, *Sol. 3*) are negligible since the outside temperature can vary of about 80 °C, according to ISO 2685. 404  
405  
406

The data collected, highlights the necessity of at least 10-12 mm thickness of thermal coating with a layer of air in between the coating and the component (around 7 mm) to reach a temperature below 250 °C. 407  
408

The model is realized considers only the conduction and not the convection as heat transfer mode in the air layer, therefore, the results reported in terms of final temperature reached can be considered conservative. Due to the articulated shape of the engine mount and to the spacers (not yet defined) used to maintain the distance in between, the convection around the structure is limited. 409  
410  
411  
412

Based on the density of the thermal coating, the mass necessary to cover the engine mount its computed ad it is equal to 8.2 kg. In order to evaluate which solution is more suitable for the engine mount this value has to be added to the mass obtained during a topology optimization at the temperature reached considering the thermal coating. 413  
414  
415  
416

The optimization is performed following the same steps as the previous optimizations. The only difference is the temperature at which the optimization is performed equal to 200 °C, in accordance with the company experience. 417  
418  
419  
420

The structure, made by Aluminum alloy (*Sol.3*), is studied, with the manufacturing constraint active in order to quantify the benefits, in terms of mass reduction and comparing them with the other materials at the same temperature. 421  
422  
423

The results showed the compliance with the requirements in terms of frequencies and stress limits and a mass reduction considerably greater than the solutions previously analyzed with *Baseline* material and *Sol.2* at the different temperatures. The final mass of the structure made by aluminium, despite of the additional mass introduced by the thermal coating, is providing a smaller mass: 47% smaller than the optimization performed with *Baseline* material in the range RT-538° and 23 % smaller than the optimizations performed with *Sol.2* in the same range of temperature. These results elected the solution made by *Sol.3* covered by the thermal coating the best candidate for the next stages of the design; therefore another TO is performed considering the complete set of sizing loads analysed separately. 424  
425  
426  
427  
428  
429  
430  
431  
432  
433  
434  
435

Load case	Torque [Nm]	Inertia [g]		
		x	y	z
1	-1277	1.5		-1
2	-1277		1.33	-1
3	-1277		-1.33	-1
4	-1277			-2

Table 3 – summary of load cases applied

The resulting structure presents an optimized design similar to the previous cases; the mass increases on average of 6%, with respect to the results performed at 200 °C considering only the vertical discrete load, due to the need of the structure to withstand loads along the x and y directions.

The natural frequencies, after the optimization, are greater than 10 Hz as requested by the problem and the stress level in each load case, analysed separately and neglecting the values in correspondence of geometrical singularities, shows a safety factor greater than 1.6.

In conclusion, the solution of the engine mount made by Aluminum alloy demonstrated to be the best, in terms of mass reduction (reaching 36% of NTE weight) and in compliance with all the constraints of the problem, therefore a final design with a CAD software is performed, following the guidelines provided by the topology optimizations.

The final design of the engine mount is reported in *Figure 12*. It has been achieved starting from the guidelines provided by the topology optimization

The proposed design tries to remain as faithful as possible to the optimized shape; some material has been added to the most stressed areas or to make the design more feasible from the manufacturing point of view. The geometry is linearly tested in order to evaluate stresses, displacements and buckling on thin reinforcements subjected to compression; in the very end, a frequency analysis is performed to evaluate the response of the structure subjected to the vertical vibration produced by the engine.

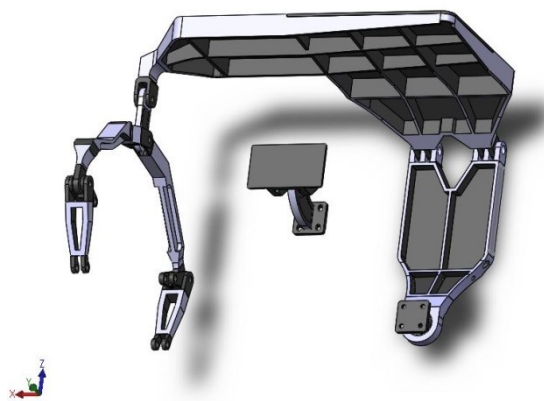
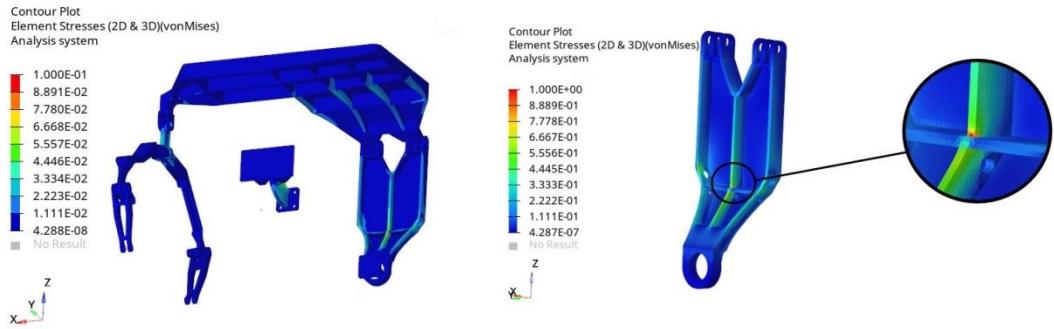


Figure 12 - Final design.

The structure is statically evaluated under the load cases presented in *Table 3*. The values reported are dimensionless on the maximum values reached.



**Figure 13 - Static analysis: element stresses of the structure under load case 4.**

The most stressed areas are located on the vertical reinforcements in the upper plate, in the lateral plate and in the connection between the Aft arms. A geometrical singularity located on the Fwd left arm is increasing the local value of stress, therefore it will be taken into consideration during the determination of the safety factor reached in the structure.

The safety coefficients with respect to the yield stress are evaluated in each static analysis and they are higher than 1.88 without considering the geometrical singularities; whereas considering them, they are higher than 1.16.

Due to the high stresses reached within the thin reinforcements of the structure, a linear buckling analysis is performed to evaluate if the phenomenon is present.

The parts on which buckling can occur are the vertical stiffeners on the upper plate, especially under the load case 1 and 4.

Load case	Buckling safety factor
1	41
2	68
3	71
4	28

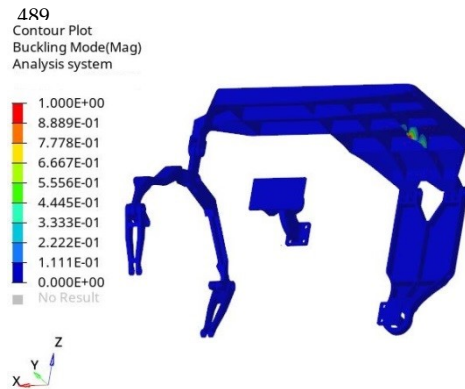


**Table 4 - Linear buckling analysis, safety factors**  
**Figure 14 - Linear buckling analysis, load case 1.**

The buckling load factor computed demonstrate that the loads are far to produce instability within the structure.

The engine mount is, also, studied under the vertical vibrating load reported by means of a modal method. The sinusoidal input signal along z-axis has to be considered as a conservative load reported in the installation manual provided by the manufacturer of the engine. The vibrating load may occur in conjunction with other discrete load cases, therefore both the effects on the structure have to be considered at the same time. Within this work, the vibrating analysis is performed, on the stressed resulting structure coming from the linear analysis performed under the load cases reported in Table 3.

The stress level in the structure is studied in correspondence of the natural frequencies to take into consideration possible undamped responses; the most stressed areas are identified and checked to guarantee that the yield stresses are not exceeded.

There are 16 natural frequencies of the structure in the range considered, in compliance with the lower limit imposed by the problem equal to 10 Hz and, at each natural frequency, the stress level is different in terms of areas and amplitude, moreover, the response is sinusoidal as the input signal

Within the range of frequency under study no resonance phenomena are present, however the vibration is producing a not negligible stress level in the structure, decreasing with frequency, higher at low frequencies and lower at high frequencies.

In the following table are reported the stress safety factors computed, considering the maximum values reached during each analysis.

Pre-stress Load case	Safety factor	Safety factor [without sin- gularities]	Pre-stress Load case	Safety factor	Safety factor [without sin- gularities]
1	0.82	1.53	1	1.23	1.91
2	1.06	1.92	2	1.56	2.38
3	1.22	2.14	3	1.76	2.69
4	0.61	1.19	4	1.02	1.70

Table 5- Safety factors during frequency analysis,  $F \leq 25\text{Hz}$  (left) and  $F > 25\text{Hz}$  (right)

The vibration is negatively impacting the safety factors, decreasing them, on average, of about 30-40% at low frequencies and about 5-10% at frequencies higher than 25 Hz.

The resulting structure demonstrated compliance with the constraints imposed by the problem in terms of mass savings, natural frequencies and stress level.

## 6. Conclusions

The present paper demonstrated that, at temperatures under 538 °C, the introduction of Titanium alloy, as an alternative to the traditional Stainless steel, guarantees a remarkable mass saving for the current design, but at temperatures above 1000 °C, the benefits obtainable were made vane since it demonstrated to violate the stress constraints, also in areas not subjected to Topology Optimization. The Stainless steel is, therefore, the most suitable material to be used in the frame of this work at high temperature despite of the high weight (135% of NTE) and stress safety factors between 1 and 1.5.

The possible benefits of introducing a fire tested thermal coating on the structure were quantified through thermal analysis, in order to define a minimum thickness to be applied to guarantee a reasonable temperature inside the engine mount.

The proposed solution demonstrated to protect the structure, reaching in the inside part less than 250 °C, with a combination of 10-12 mm thermal coating thickness spaced by 10 mm of air cavity from the engine mount allowing, therefore, to investigate the use of Aluminum alloy, unconventional choice for this type of application.

After being Topology Optimized and despite of the additional weight introduced by the thermal coating, this Aluminum alloy solution demonstrated to produce the greater mass saving. The final mass is, in fact, 47% smaller than the one obtainable with Stainless steel and 23 % smaller than the one obtainable with Titanium alloy, in the range RT-538 °C, including the masses of the thermal coating and connections.

The Aluminium alloy structure, once optimized with the complete set of sizing loads, was used as guideline to produce the final design of the engine mount with the purpose of manufacturing it with conventional metal cutting techniques. The result, tested in the very end under linear (static and buckling) and frequency analysis, demonstrates compliance with the constraints imposed by the problem in terms of mass saving, natural frequency, stresses and accessibility.

### Considerations on the possible causes of error:

- **Simplification of the model:** the engine mount has been redesigned at the beginning of the work, with the same interfaces towards the engine and with the same bolts, in accordance with the preliminary design, however, before starting the optimization campaign, those details have been simplified in order to lighten the computational cost during this work. This approximation is neglecting a considerable mass in the model that may affect the modal analysis and the frequency analysis in the final design; moreover, the model is neglecting their natural elasticity, without introducing further d.o.f. in the structure.

• **Load cases:** within the first optimization campaign only one load case has been considered; this fact has led to not fully realistic structures, where the structure would not be able to support the discrete load case along the x-axis, however, this is not affecting the result of the campaign itself since all the solutions have been compared starting from the same load inputs. Within this work, the longitudinal thrust from the exhaust gases, has been neglected due to its small value.

• **Geometrical singularities:** few geometrical singularities in the geometry led to correspondent singularities in the stress values. However, as demonstrated by the stress safety factors computed, they are not impacting the results of this work and they will be removed before freezing the design of the engine mount.

• **Stress and displacement values:** stresses and displacements computed within the TO, may be affected by errors; in fact, they are overestimating the real values due to the presence of elements with intermediate densities; a further static analysis could be performed after the *Osmooth* function in each optimization, but this was out of the scope of the work since a final design with CAD software was planned to be performed.

• **Material Properties:** the material properties found in the literature are one of the key inputs of this work, especially in the first optimization campaign. Many data are available for the materials selected up to around 500 °C, but they are not enough to produce trustable conclusions on the behavior of the materials at 1100 °C, in compliance with the ISO 2685. At this temperature, the materials are not characterized using common tensile tests, but more likely using compressive tests, in order to evaluate their manufacturability once heated. Compressive tests results, therefore, have been adopted in the first optimization campaign, with the hypothesis of isotropic material. Moreover, a lack in compressive test results performed on *Baseline* material forced to consider another material with characteristics as close as possible to the initial one over the entire temperature range considered, in order to make a reasonable comparison: the 17-7 PH stainless steel.

Another consideration that must be pointed out is the strong dependency of the compressive test properties with respect to the strain rate during test; leading to great differences in results; in this work both the 17-7 PH stainless steel and the Titanium alloy have been used taking into considerations the same strain rate during compressive tests.

• **Volume fraction constraint:** during the optimizations has been set a minimum volume fraction reachable by the solver, in order to avoid the exclusion or relevant connections of the engine mount such as the Aft arms.

• **Structural damping:** During the frequency analysis, the structural damping is neglected leading to possible small discrepancies in the results of a few percentage points.

• **Convection heat transfer mode:** During the thermal analysis performed on the structure the convection has been neglected in the space between the thermal coating and the structure, considering only conduction as heat transfer mode; this choice has been done considering that the articulated shape of the engine mount and the spacers used to maintain the correct air layer thickness would not facilitate the presence of convective motions. The results of the temperature reached are therefore conservative.

## Funding

“This research was funded by the Clean Sky 2 Joint Undertaking under the European Union’s Horizon 2020 research and innovation programme



**Conflicts of Interest:** the authors declare no conflict of interest.

**References**

- [1] <https://www.cleansky.eu> 595
- [2] <https://www.leonardocompany.com/it/products/aw609> 596
- [3] Razvan Cazacu, Lucian Grama, Overview of structural topology optimization methods for plane and solid structures, Annals of University of Oradea, Fascicle of Management and Technological Engineering, Issue #3, December 2014, <http://www.imtuoradea.ro/auo.fmte/> 597
- [4] Peter W.Christensen, Anders Klarbring, An Introduction to Structural Optimization, 2009, Springer, ISBN 978-1-4020-8665-6. 598
- [5] Altair, Practical Aspects of Structural Optimization - a study guide, third edition,2018. 599
- [6] ARMCO® PH 13-8 Mo STAINLESS STEEL product data bulletin, <https://www.aksteel.nl/> 600
- [7] BS ISO 2685,1998 Aircraft – Environmental test procedure for airborne equipment – Resistance to fire in designated fire zones, British Standards Institution. 601
- [8] Properties and processing of TIMETAL® 6-4, Titanium metals corporation, USA, 1998. 602
- [9] Metallic Materials Properties Development and Standardization (MMPDS) - 4, FAA, 2009. 603
- [10] [https://2020.help.altair.com/2020/hwsolvers/os/topics/solvers/os/dtpl\\_bulk\\_r.htm?zoom\\_highlightsub=MINdim](https://2020.help.altair.com/2020/hwsolvers/os/topics/solvers/os/dtpl_bulk_r.htm?zoom_highlightsub=MINdim) 604
- [11] Alloy 13-8, technical Datasheet, <WWW.neonickel.com> 605
- [12] <https://www.cleansky.eu/sites/default/files/inline-files/CS2-FRC-Cfp09%20Final.pdf> 606
- [13] Shibayan Roy, Satyam Suwas, The influence of temperature and strain rate on the deformation response and microstructural evolution during hot compression of a titanium alloy Ti–6Al–4V–0.1B; 2012, [www.elsevier.com/locate/jalcom](http://www.elsevier.com/locate/jalcom). 607
- [14] M. Zeinali, E. Shafiei, R. Hosseini, Kh. Farmanesh, A.R. Soltanipoor and E. Maghsodi; Hot Deformation Behavior of 17-7 PH Stainless Steel; Iranian Journal of Materials Forming, Vol. 4, No. 1, pp 1-11, 2017. 608

617